

Neutronic assessment of the IFMIF-DONES HFTM specimen stack distribution

I. Álvarez^{a,*}, M. Anguiano^a, F. Mota^b, R. Hernández^c, Y. Qiu^d

^a Department of Atomic, Molecular and Nuclear Physics, University of Granada, UGR, Granada, Spain

^b Laboratorio Nacional de Fusión por Confinamiento Magnético, CIEMAT, Madrid, Spain

^c División de Materiales de Interés energético, CIEMAT, Madrid, Spain

^d Karlsruhe Institute of Technology, KIT, Karlsruhe, Germany

ARTICLE INFO

Keywords:

IFMIF-DONES
HFTM
Neutronics
DPA
Comparative

ABSTRACT

IFMIF-DONES (International Fusion Materials Irradiation Facility- DEMO Oriented NEutron Source) is a neutron irradiation facility designed to collect data on material irradiation for the construction of demonstration fusion power plants.

This study focuses in investigate the effect of a realistic model of specimens being irradiated in HFTM in IFMIF-DONES, and its comparison with previous results with the homogeneous model. Neutron fluence rate, damage dose rates, and gas production have been calculated for the standard $20 \times 5 \text{ cm}^2$ profile and a $10 \times 5 \text{ cm}^2$ beam size. These calculations were performed for a deuteron beam with an energy of 40 MeV and a current of 125 mA. More realistic neutronics model gives very consistent DPA volumes with the previous. The main difference is a neutron slight streaming in the detailed one. The distribution of DPA shows irregular patterns depending on specimen location. This research highlights the significant role played by specimen distribution in enhancing the accuracy and reliability of dpa measurements within the IFMIF-DONES facility and the influence of the beam size.

1. Introduction

The International Fusion Materials Irradiation Facility-DEMO Oriented NEutron Source (IFMIF-DONES) [1–3] is a neutron irradiation facility based on the stripping $d\text{-Li}$ neutron source to produce high energy neutrons at sufficient intensity to irradiate materials under similar irradiations conditions to the ones expected in the future nuclear fusion reactors such as the DEMOnstration fusion power plant (DEMO). Its purpose is to provide essential irradiation material data to qualify materials for DEMO. Within IFMIF-DONES, only one of the IFMIF-DONES accelerators, operating at 40 MeV and 125 mA, is utilised, specifically in conjunction with the High Flux Test Module (HFTM) for material specimen irradiation. The HFTM plays a crucial role in fulfilling the mission of DONES by supplying material irradiation data.

The desired primary displacement damage dose, measured in Displacements Per Atom (DPA), for the design of the DEMO first wall is 20 dpa in the initial phase, based on the Norgett, Robinson and Torrens (NRT) model of primary displacement damage [4], and 50 dpa in the second phase. The DONES HFTM has specific top-level requirements,

aiming to achieve a 0.3 Liter irradiation volume with 20–30 dpa in less than 2.5 years (R-1), and a 0.1 Liter volume with 50 dpa in less than 3 years (R-2). The previous nuclear response analyses had been calculated with homogeneous rigs in the HFTM [5], considering 75 % EUROFER-97 and 25 % natural sodium. In this work, the data is obtained with a detailed specimen distribution in each rig of the HFTM, the CLC.v1.0 model, acronyms of Capsule Loading Configuration, shown in Fig. 1. Additionally, the possibility of concentrating the deuteron beam from a standard footprint of $20 \times 5 \text{ cm}^2$ to a reduced size of $10 \times 5 \text{ cm}^2$ to achieve higher damage rates on the center specimen capsules is being considered. However, the irradiation performance of these two beam sizes has not been fully analysed thus far. Therefore, this paper presents the modelling and nuclear response analyses of the updated rigs in the HFTM.

This paper compares the neutron fluence rate, the primary displacement damage and the gas production ratio considering two kinds of models of the packaging of the HFTM specimen stack, the homogeneous HFTM specimen stack and the CLC.v1.0 model.

* Corresponding author.

E-mail address: iac@ugr.es (I. Álvarez).

<https://doi.org/10.1016/j.fusengdes.2024.114212>

Received 10 November 2023; Received in revised form 22 January 2024; Accepted 28 January 2024

Available online 6 February 2024

0920-3796/© 2024 The Author(s). Published by Elsevier B.V. This is an open access article under the CC BY-NC-ND license (<http://creativecommons.org/licenses/by-nc-nd/4.0/>).

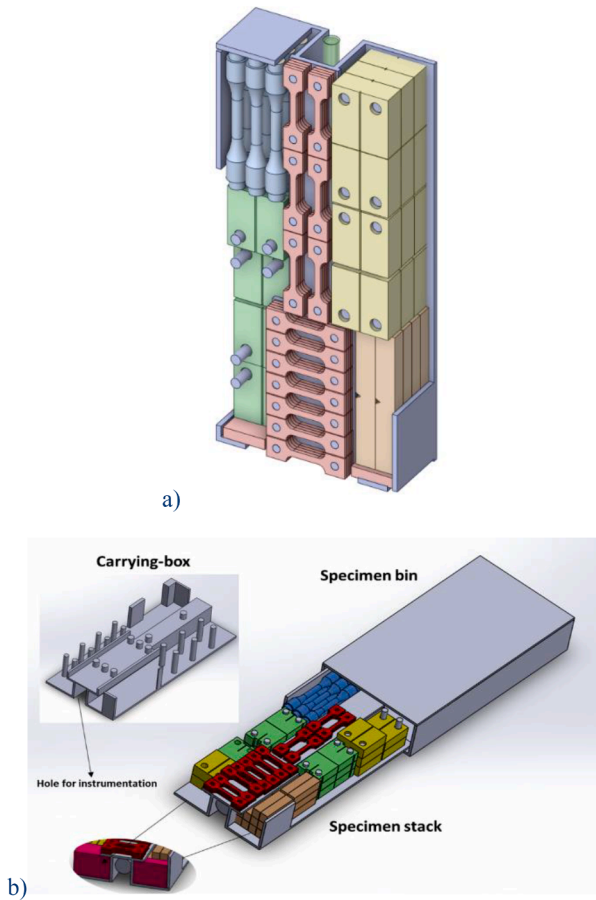


Fig. 1. Packaging proposal of SSTS in the HFTM specimen stack a) capsule with the SSTS installed; b) How the specimen stack is assembled into the Specimen bin [7].

2. Methodology

2.1. Materials and methods

The specimen distribution CLC.v1.0 used for the calculation contains five different types of EUROFER-97 specimens. They were designed with Small Specimen Test Techniques (SSTS) to ensure the maximum number of specimens in the space available. This packaging proposal assessed the number of specimens per rig, depending on the mechanical tests, are 52 flat tensile, 9 cylindrical fatigue, 12 KLST impact (ISO 14,556 standard, Annex D), 17 Fatigue Crack Growth (FCG) and 11 Fracture Toughness (FT), Table 1. Moreover, the model has blocks to reduce the minimum free space in the specimen stack, and this model has the minimum number of specimens for each type of test and capsule to characterise the damage [6].

This model has 48.16 % of Eurofer-97 samples and 39.87 % of sodium, in total 82 % of the specimen bin total volume. For the simulation, the central hole has a diagnostic, leaving everything else void. The diagnostic placed is a Self Powered Neutron Detector (SPND). The materials considered for the SPND have been rhodium for the emitter, alumina for the insulator and inconel600 for the collector.

The specimen stack CAD model has been simplified to adapt it to the neutronics requirements using the SpaceClaim 2021 R1 Software [8]. The criteria used for the simplification was to keep the original volume of the specimens. The simplified model was converted into Monte Carlo N-Particles (MCNP6.2) [9] model using SuperMC V3.2 [10,11]. An individual model was obtained for each capsule of the HFTM, and next, they were installed in the whole model of the HFTM in each specific location. Horizontal cross-section of the MCNP model of the HFTM with

Table 1

Different kinds of SSTS depending on the mechanical test needed to characterise the irradiation damage.

Type	Figure	Volume [cm ³]	Units/rig	Total units
Tensile		0.0298	52	1664
Fatigue		0.1948	9	288
FCG		0.2835	17	544
FT		0.5686	11	352
KLST		0.3223	12	384
				3232

the detailed model of the specimen stack installed is shown in Fig. 2. The MCNP Test Cell (TC) model used is the “mdl9.2.0” version. This model is an updated version of the described on [5].

2.2. Simulation methodology

The McDeLicious code vision 2017 has been employed for neutron and photon generation and transport calculations [12]. McDeLicious is

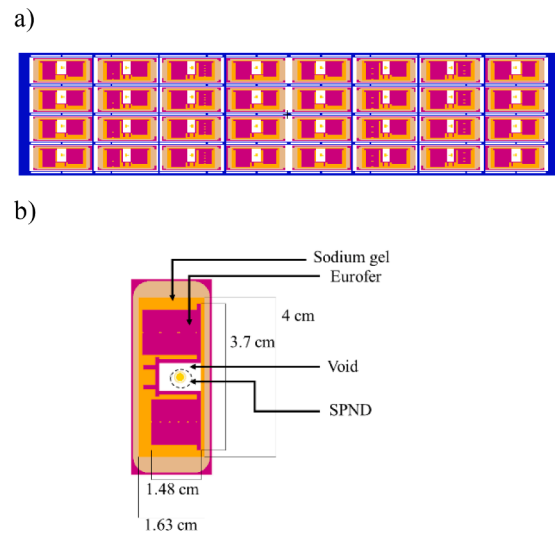


Fig. 2. a) Horizontal cross-section of the MCNP model of the HFTM with the detailed model of the specimen stacks installed; b) Horizontal cross section of one specimen stack.

an extension of MCNP 6.2 code [9] with the ability to reproduce the stripping $d + {}^6,7\text{Li}$ neutron source [13]. FENDL3.1d [14] nuclear data libraries are used for neutron transport calculations, while the photon transport calculations were made using mcplib84 [15].

The primary displacement damage induced by neutrons has been calculated using two methodologies, the NRT methods [4] and arc-dpa method [16].

The design of equivalent neutron irradiation experiments had been based on the determination of radiation level using the NRT model. In this methodology, only four elements were adjusted, Cu, Fe, Au and W, and it takes into account neither the recombination nor clustering formation [4]. Recently, a new dpa concept was developed in the framework of the IAE CRP project “Primary Radiation Damage Cross Sections”, the named arc-dpa method. This method to determine the displacement damage takes into account the recombination of defects during the thermal spike because they are fitted with molecular dynamics calculations for a wide range of elements involved in nuclear fusion development [16]. However, it is essential to continue using the NRT model to compare with previous calculations and add the new concept arc-dpa to generate the new primary displacement damage dose database. The nuclear data library used to determine the NRT and arc-dpa primary displacement damage is JEFF3.3DPAarc [16].

In addition, the He and H production rates have also been calculated because helium and hydrogen production to damage dose ratios directly impact on the diffusion of defects and the evolution of damage tracks [17]. Throughout this paper, the He and H production to damage dose ratios will be referred to as He and H ratios, respectively, for simplicity.

The deuteron beam dynamic used is the IFMIF/EVEDA profile [1], with a footprint area of $20 \times 5 \text{ cm}^2$ and $10 \times 5 \text{ cm}^2$. The materials irradiation doses have been calculated considering 345 days of full power of operation because 20 days of maintenance were considered [18].

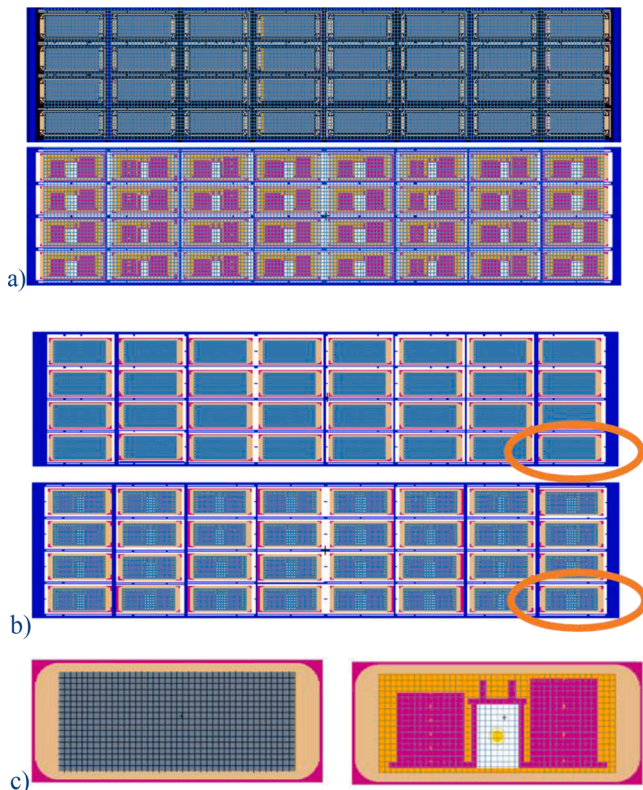


Fig. 3. Horizontal cross section of the HFTM; a) Specimens region mesh for the h.m. and CLC.v1.0 models. b) Specimens stacks mesh for the h.m. and CLC.v1.0 models. c) Mesh zoom in the highlight part of b).

Two meshes were used to tally the results. One that covers all the HFTM (Fig. 3a), specimen region mesh (i), and the other only covers the volume in the rigs avoiding the structural parts of HFTM, specimen stack mesh (Fig. 3b) (ii). A zoom of this mesh is shown in Fig. 3c. The specimen region mesh (i) has a resolution of $2.5 \times 2.5 \times 2.5 \text{ mm}^3$, while the specimen stack mesh (ii) $1.0 \times 1.0 \times 1.0 \text{ mm}^3$. In this paper, the outcomes obtained for these two beam sizes are contrasted with the homogeneous and detailed rigs model (CLC.v1.0). Moreover, cell tallies have been used for the calculation of different parameters in the specimens cells for the detailed model (iii). In this case only the volume of the specimens is taken into account.

The statistic relative error of meshtals and tallies are lower than 0.05. Unless otherwise specified, the cross-sectional views presented in the subsequent figures depict either the X-Y plane at the beam level or the X-Z plane intersecting the center of the target.

3. Results

This section compares the neutron fluence rates, the primary displacement damage rates, and the gas production (He and H) to displacement damage dose ratios obtained for both models assessed.

3.1. Neutron fluence rate

The horizontal cross sections of the neutron fluence rate maps [$\text{ncm}^{-2}\text{s}^{-1}$] at the middle of the deuteron beam for a) $20 \times 5 \text{ cm}^2$ and b) $10 \times 5 \text{ cm}^2$ footprint size is shown in Fig. 4. The central four compartments typically experience a neutron flux ranging from 1 to $5 \times 10^{14} \text{ ncm}^{-2}\text{s}^{-1}$. The flux distribution in the HFTM is asymmetric due to the 9° incident angle of the deuteron beam, which is maintained in DONES. Using the detailed specimen stack model, CLC.v1.0, neutron streaming can be appreciated in the central part of the rigs where the diagnostic is located. Besides, comparing the $20 \times 5 \text{ cm}^2$ and $10 \times 5 \text{ cm}^2$ footprint maps, it is observed that the neutron fluence rate increases in the two central columns of specimen stacks.

The neutron fluence rate maps for the HFTM homogeneous specimens stack are shown in Fig. 5. Slight differences are found in the neutron fluence rates between both models, homogeneous and detailed specimen stacks. The more significant difference is the slight neutron streaming observed between the specimen stacks.

The statistic relative error is given in Fig. 6. It is shown for a $20 \times 5 \text{ cm}^2$ beam footprint and for the two models. As expected, uncertainties are lower in the region where neutron fluence is higher and vice versa. In any case, uncertainties are between 0.2 and 1 %, indicating that they are small enough throughout the entire area of interest [9].

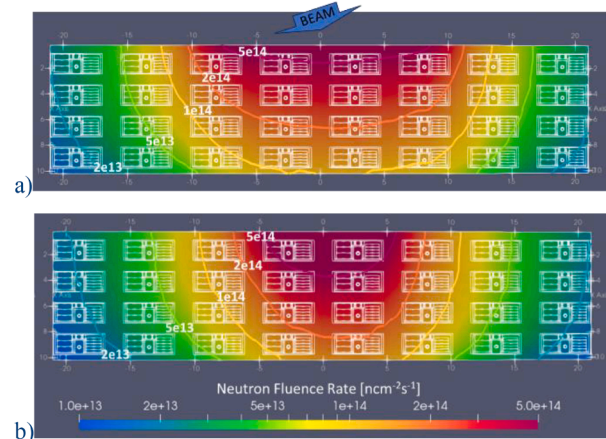


Fig. 4. Horizontal cross section of the Neutron fluence rate maps [$\text{ncm}^{-2}\text{s}^{-1}$] of the detailed specimen stacks at the middle of the deuteron beam; a) $20 \times 5 \text{ cm}^2$ and b) $10 \times 5 \text{ cm}^2$ footprint size.

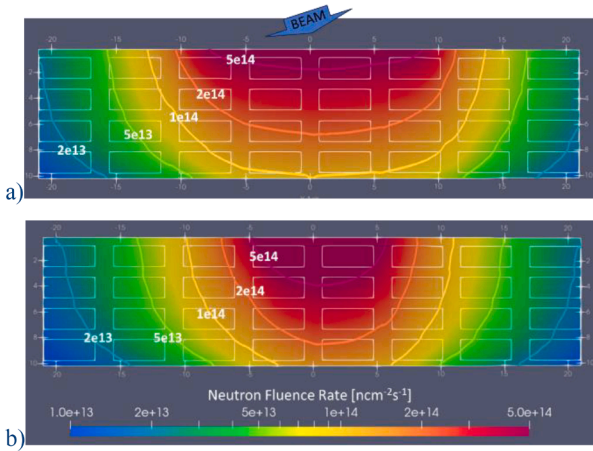


Fig. 5. Horizontal cross section of the Neutron fluence rate maps [$\text{ncm}^{-2}\text{s}^{-1}$] of the homogeneous specimen stacks at the middle of the deuteron beam; a) $20 \times 5 \text{ cm}^2$ and b) $10 \times 5 \text{ cm}^2$ footprint size.

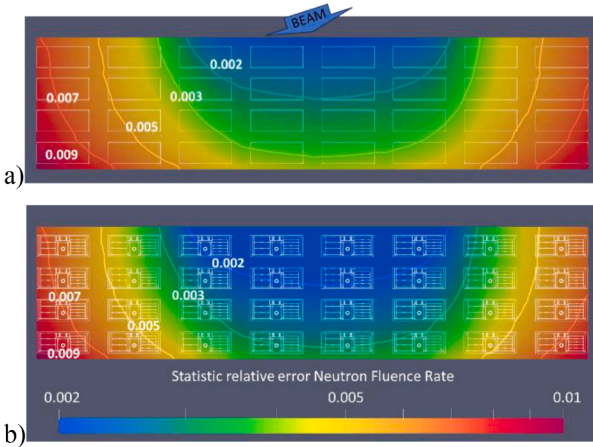


Fig. 6. Horizontal cross section of the statistic relative error of the neutron fluence rate maps of the two models at the middle of the $20 \times 5 \text{ cm}^2$ deuteron beam footprint size.

The differences in the neutron fluence rate using different packaging configuration can be appreciate in Fig. 7. The white lines correspond to the results for the homogeneous model and the coloured lines for the

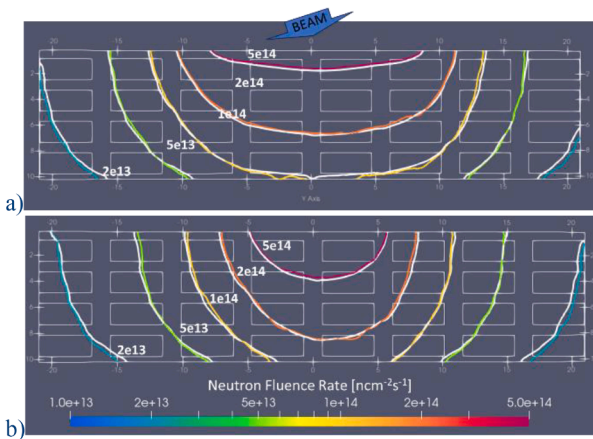


Fig. 7. Horizontal cross section of the neutron fluence rate maps [$\text{ncm}^{-2}\text{s}^{-1}$] of the two models at the middle of the deuteron beam: white lines-h.m. and colour lines -CLC.v1.0; a) $20 \times 5 \text{ cm}^2$ and b) $10 \times 5 \text{ cm}^2$ footprint size.

CLC.v1.0 one. There are five isobar lines with their neutron fluence rate value.

3.2. Primary displacement damage ratio

The achievement of the required primary displacement damage rate performance in the HFTM is crucial to fulfil the objectives of DONES. The primary displacement damage rate is represented in dpa per full power year (dpa/fpy). The primary displacement damage obtained is the equivalent iron displacement damage calculated by integrating the neutron flux with the natural iron DPA production cross section. As commented above, the primary displacement damage has been calculated using both methodologies, NRT model and arc-dpa model.

Primary displacement damage rate horizontal cross section maps calculated in the middle of the deuteron beam for both footprint sizes and for both dpa concepts are shown in Figs. 8 and 9. In them can be seen with the isobar lines that the NRT_dpa rate is from 28 to 5 dpa/fpy for the $20 \times 5 \text{ cm}^2$ footprint and 46 to 5 dpa/fpy for the $10 \times 5 \text{ cm}^2$ footprint.

The available integrated irradiation volume (32 rigs) versus primary damage dose rate [NRT_dpa/fpy] for the different specimens stacks model (homogeneous and CLC.v1.0), considering a footprint of $20 \times 5 \text{ cm}^2$ is shown in Fig. 10a) and b) for the footprint of $10 \times 5 \text{ cm}^2$. In these figures, the available irradiation volume is compared according to the primary displacement damage obtained, taking into account different volumes. These volumes are referenced to the meshes and tally defined in Section 2.2. The first two areas are calculated from the whole available volume to irradiate specimens in the HFTM (mesh i); in the next two areas, the mesh is adjusted to the areas of the specimen stack (mesh ii), while the fifth area corresponds only to the volume of the specimens in the CLC.v1.0 model (tally iii). The solid lines refer to the homogeneous model, while the dashed and dotted lines refer to the CLC.v1.0 model. It can be seen how the available volume with a specific number of DPAs decreases, making the high-DPA volume extremely important to be fully utilized. Another significant observation from these figures is that the available volume with a specific dpa value is lower in the detailed model CLC.v1.0 model. Besides, if it is considered only the volume of the sample of the CLC.v1.0 model, the total specimen volume decreases significantly. That does not mean that this sample payload will be the only option for HFTM, it provides us an indication to optimize the payload and increase the utilized volume.

In Fig. 11 the available integrated irradiation volume is shown versus the primary damage dose rate [arc-dpa/fpy] for the same cases have been used as for NRT_dpa. It can be seen that the behaviour is the same,

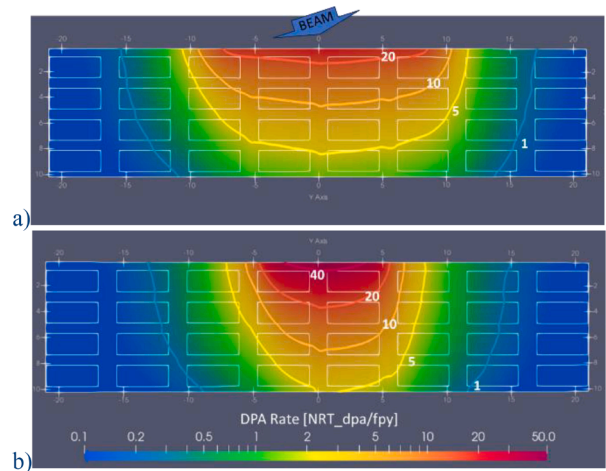


Fig. 8. Horizontal cross section of the primary displacement damage ratio [NRT_dpa/fpy] of the homogeneous specimen stacks at the middle of the deuteron beam; a) $20 \times 5 \text{ cm}^2$ and b) $10 \times 5 \text{ cm}^2$ footprint size.

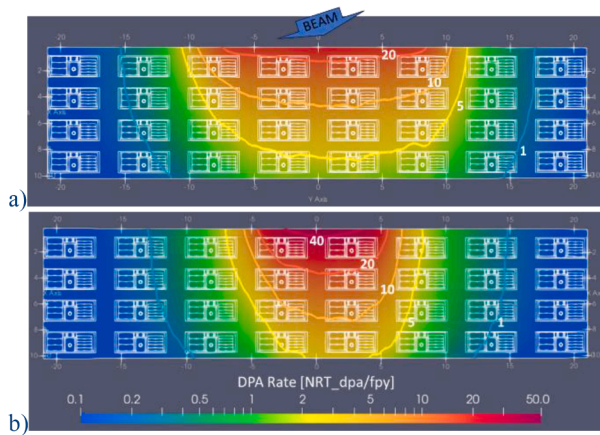


Fig. 9. Horizontal cross section of the primary displacement damage ratio [NRT_dpa/fpy] of the CLC.v1.0 specimen stacks at the middle of the deuteron beam; a) $20 \times 5 \text{ cm}^2$ and b) $10 \times 5 \text{ cm}^2$ footprint size.

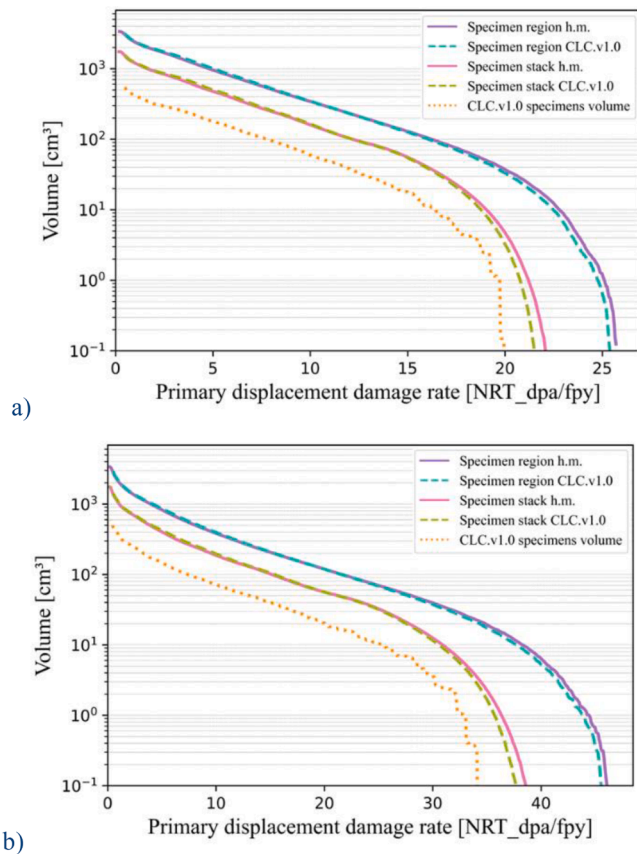


Fig. 10. Available integrated irradiation volume (32 rigs) versus primary damage dose rate [NRT_dpa/fpy] for the different specimens stacks model (homogeneous and detailed); a) $20 \times 5 \text{ cm}^2$ and b) $10 \times 5 \text{ cm}^2$ footprint size.

but the range of values for the arc-dpa is smaller than for the NRT_dpa, being a maximum of 8 for the standard beam and 14 for the reduced beam. As commented above, it is due to the arc-dpa model take into account recombination processes during the thermal spike.

The primary displacement damage criteria outlined in Section 1 for DONES can be translated into two high level specific requirements: R-1, which calls for achieving 8–12 NRT_dpa/fpy in a volume of 0.3 Liters, and R-2, which aims for 16.7 NRT_dpa/fpy in a volume of 0.1 Liters. Considering the five different scenarios shown in previous Figs. 10 and

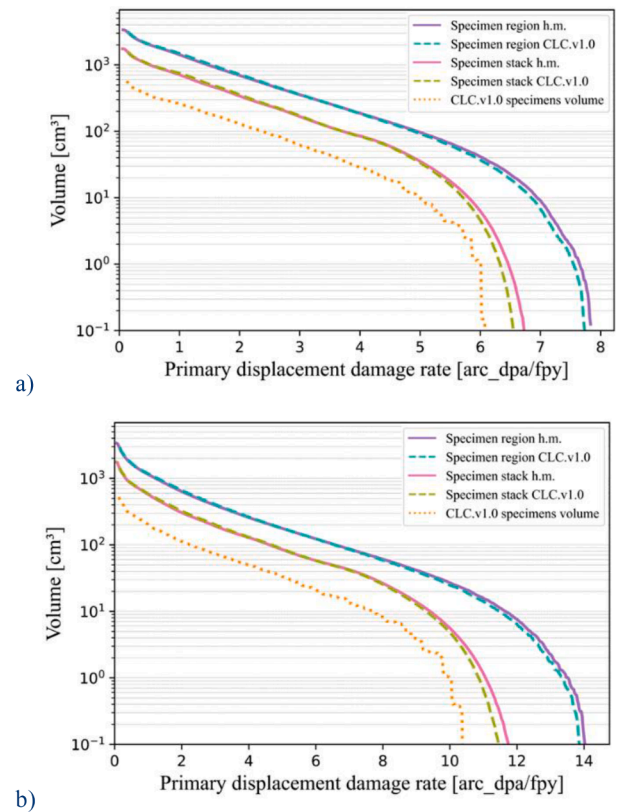


Fig. 11. Available integrated irradiation volume (32 rigs) versus primary damage dose rate [arc-dpa/fpy] for the different specimens stacks model (homogeneous and detailed); a) $20 \times 5 \text{ cm}^2$ and b) $10 \times 5 \text{ cm}^2$ footprint size.

11, the volumes that meet the two requirements for both the standard and reduced beam sizes have been calculated. The first scenario involves the homogeneous model using the (i) mesh. The second scenario utilises CLC.v1.0 model with the (i) mesh. The third scenario employs the homogeneous model with the (ii) mesh, which covers only the area of the 32 rigs. The fourth scenario utilises the (ii) mesh, covering the rigs, along with the CLC.v1.0 model. Lastly, the fifth scenario considers only the volume occupied by the specimens in CLC.v1.0 model (tally iii). The volume results are shown in Table 2. For the homogeneous and detailed models and the $20 \times 5 \text{ cm}^2$ footprint, the R-1 and R-2 are fulfilled considering the specimens region. The reduced beam footprint $10 \times 5 \text{ cm}^2$ fulfil only the R-2 for both models. It is worth to note that considering different references when calculation the DPA volume requirements can lead to a reduction in the calculated values, since the available volume is lower and then, direct comparison with the high level requirements does not proceed.

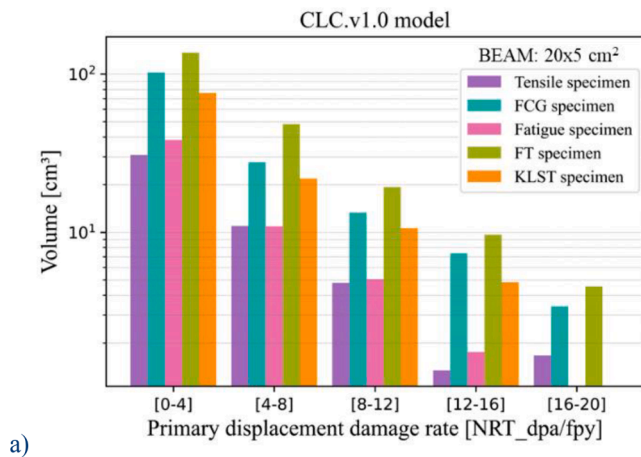
A volume histogram based on the achieved primary displacement damage has been obtained as a function of the different kinds of samples of the CLC.v1.0 model and the two beam sizes.

Fig. 12 shows the histogram of the amount of available volume per type of sample as a function of the amount of dpa received, according to the NRT_dpa damage model. The decrease in volume is not uniform and therefore there are no samples available at high dpa. On the other hand, Fig. 13 shows the histogram of the number of samples by type as a function of the dpa. These figures show that the specimens types are not uniformly distributed along with the dpa level that they are going to receive. For the case of arc-dpa, the histograms are equivalent in behaviour, but with the maximum values of dpa being lower. Then, from these figures, it is concluded that it would be interesting to study how to reconfigure the sample location in order to distribute the dpa values more homogeneously for the different types of specimens.

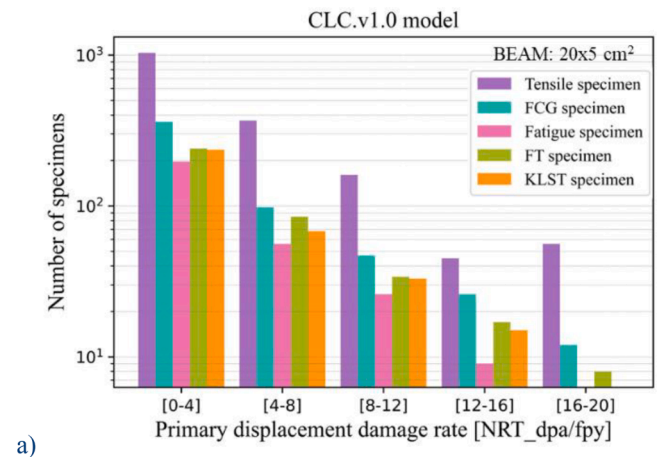
Table 2

Volume [litre] available in the NRT_dpa ranges of R-1 and R-2 depending on the model and volume under consideration. Uncertainties are lower than 0.3 % in all the cases.

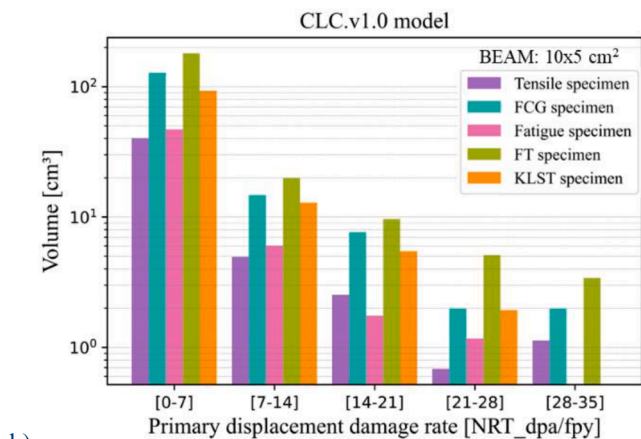
Volume DPA requirements [L]	Target value	Specimens region h. m.		Specimens region CLC.v1.0		Specimens stack h. m.		Specimens stack CLC.v1.0		CLC.v1.0 specimens volume	
		20 × 5	10 × 5	20 × 5	10 × 5	20 × 5	10 × 5	20 × 5	10 × 5	20 × 5	10 × 5
Beam											
R-1 8–12 NRT_dpa/fpy	0.3	0.27	0.20	0.29	0.22	0.14	0.10	0.15	0.10	0.056	0.036
R-2 >16.7 NRT_dpa/fpy	0.1	0.089	0.17	0.085	0.17	0.03	0.08	0.03	0.08	0.008	0.032



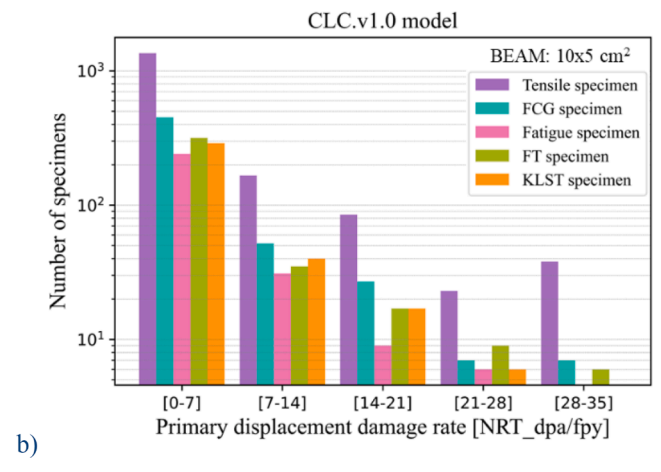
a)



a)



b)



b)

Fig. 12. Histogram of available irradiation volume by type demonstrates versus primary damage dose rate [NRT_dpa/fpy] for the CLC.v1.0 model; a) $20 \times 5 \text{ cm}^2$ and b) $10 \times 5 \text{ cm}^2$ footprint size.

3.3. Gas production to displacement damage ratio

As commented above, the gas production demonstrates a synergistic effect with DPA, directly influencing the diffusion of damage defects [17]. In this case, the He/dpa ratio in units of [He appm/dpa_NRT], considering the volume of the HFTM with specimens and the model with homogeneous rigs, as well as solely considering the volume of the specimens have been calculated and shown in Fig. 14. Furthermore, this calculation only takes into account data from centrally located rigs, 16 in total. As observed, for a $20 \times 5 \text{ cm}^2$ beam, the peak data points fall within the range of 14 He-appm/dpa, which is quite close to the expected range of 11–12 He appm/dpa for DEMO [19,20]. In Fig. 15 the ratio H-appm/dpa is shown, in this case the high part of the volume is around 55 and 60 H-appm/dpa, while in DEMO the values expected are between 45 and 55 H-appm/dpa [19,20]. Considering the ratios for the

Fig. 13. Histogram of the number of available samples by type versus primary damage dose rate [NRT_dpa/fpy] for the CLC.v1.0 model; a) $20 \times 5 \text{ cm}^2$ and b) $10 \times 5 \text{ cm}^2$ footprint size.

CLC.v1.0 specimens cell tallies, the volume around the expected values for DEMO are very much lower than the specimen region CLC.v1.0 for the production of He and H. Maybe considering other specimens distribution, these ratios can be adapted in order to reach the values expected in DEMO.

4. Conclusions

Neutron transport calculations have been performed to study how the irradiation parameters change in the HFTM specimen area as a function of model heterogeneity and mesh approach. A detailed model of the HFTM specimen stacks (CLC.v1.0) has been modelled with this goal. Therefore, the irradiation parameters obtained using the homogeneous HFTM model (previously used in IFMIF-DONES project) and the CLC.v1.0 have been compared. The irradiation parameters compared are neutron fluence rate, the primary displacement damage, according

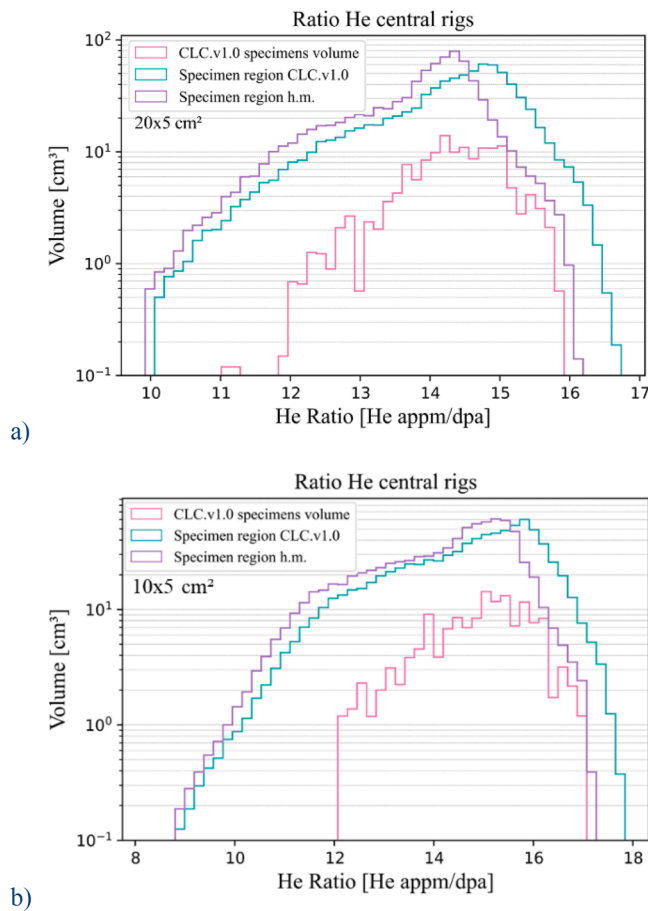


Fig. 14. Irradiation volumes as function of He-DPA ratio. Using a) $20 \times 5 \text{ cm}^2$ and b) $10 \times 5 \text{ cm}^2$ footprint size.

to the NRT_dpa and arc-dpa models, and gas production, He and H, ratio. Also, two beam footprint sizes have been considered, the standard $20 \times 5 \text{ cm}^2$ and the reduced $10 \times 5 \text{ cm}^2$.

The principal difference in neutron fluence rates between the homogeneous and detailed models is a neutron slight streaming in the detailed one, due to the differences in the packaging. This study has provided valuable insights into the target volumetric values for the primary displacement damage rates and their alignment with specific requirements. It has been established that a beam size of $20 \times 5 \text{ cm}^2$ is optimal for satisfying R-1 and R-2. With a beam size of $10 \times 5 \text{ cm}^2$, R-2 is amply satisfied, while R-1 is not fulfilled. Moreover, the distribution of specimens according to the primary displacement damage level is not homogeneous. Finally, with respect to the gas production ratio, values are obtained in the DEMO line. The amount of cubic centimetres in these ratios is low if only the CLC.v1.0 specimens volume is taken into account.

Furthermore, the inclusion of specimen samples distributed within the rigs of the model has introduced a higher degree of heterogeneity into the dataset. This finding underscores the importance of specimen distribution as a significant factor influencing data variability within the study. And it is not just about moving from a homogeneous design to a more detailed one, but about how the payload of the samples can be optimised, e.g., on which primary displacement damage dose will receive, and how many of each type are needed per dpa and with desired doses.

These conclusions contribute to a better understanding of the factors impacting upon primary displacement damage distribution along the specimens and provide guidance for the design and distribution of the specimens inside the rigs of the HFTM in the IFMIF-DONES facility.

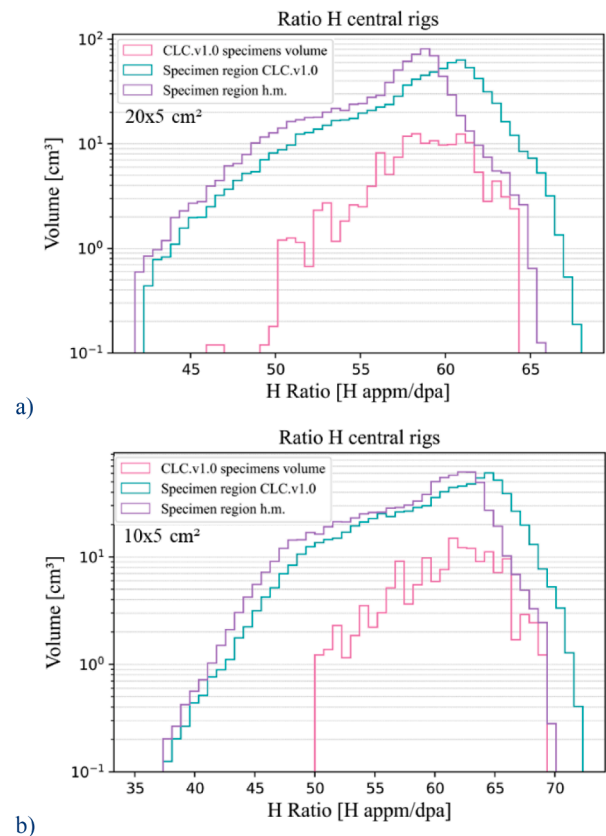


Fig. 15. Irradiation volumes as function of H-DPA ratio. Using a) $20 \times 5 \text{ cm}^2$ and b) $10 \times 5 \text{ cm}^2$ footprint size.

CRediT authorship contribution statement

I. Álvarez: Data curation, Investigation, Methodology, Software, Validation, Writing – original draft, Writing – review & editing. **M. Anguiano:** Funding acquisition, Investigation, Methodology, Project administration, Supervision, Validation, Writing – original draft, Writing – review & editing. **F. Mota:** Conceptualization, Funding acquisition, Methodology, Software, Supervision, Validation, Writing – original draft, Writing – review & editing. **R. Hernández:** Resources. **Y. Qiu:** Conceptualization, Resources, Supervision.

Declaration of competing interest

The authors declare that they have no known competing financial interests or personal relationships that could have appeared to influence the work reported in this paper.

Data availability

The authors do not have permission to share data.

Acknowledgments

This work has been supported by the European Union's FEDER program, IFMIF-DONES Junta de Andalucía's program at the Universidad de Granada, by MCIN/AEI/10.13039/501100011033/FEDER, UE (PID2022-137543NB-I00) and has been carried out within the framework of the EUROfusion Consortium, funded by the European Union via the Euratom Research and Training Programme (Grant Agreement No 101052200 — EUROfusion). Views and opinions expressed are however those of the author(s) only and do not necessarily

reflect those of the European Union or the European Commission. Neither the European Union nor the European Commission can be held responsible for them.

References

- [1] J. Knaster, A. Ibarra, J. Aba, A. Abou-Sena, F. Arbeiter, et al., The accomplishment of the engineering design activities of IFMIF/EVEDA: the European–Japanese project towards a Li(d,xn) fusion relevant neutron source, *Nuclear Fusion* 55 (2015) 086003, 30pp.
- [2] A. Ibarra, R. Heidinge, P. Barabaschi, F. Mota, A. Mosnier, P. Cara, F.S. Nitti, A stepped approach from IFMIF/EVEDA toward IFMIF, *Fusion Sci. Technol.* 66 (2014) 252–259.
- [3] D. Bernardi, F. Arbeiter, M. Cappelli, U. Fischer, A. García, et al., Towards the EU fusion-oriented neutron source: the preliminary engineering design of IFMIF-DONES, *Fusion Eng. Design* 146 (2019) 261–268.
- [4] M.J. Norgett, M.T. Robinson, I.M. Torrens, A proposed method of calculating displacement dose rates, *Nucl. Eng. Des.* 33 (1975) 50–54, [https://doi.org/10.1016/0029-5493\(75\)90035-7](https://doi.org/10.1016/0029-5493(75)90035-7).
- [5] Y. Qiu, F. Arbeiter, U. Fischer, F. Schwab, IFMIF-DONES HFTM neutronics modeling and nuclear response analyses, *Nuclear Mater. Energy* 15 (2018) 185–189, <https://doi.org/10.1016/j.nme.2018.04.009>.
- [6] Y. Qiu, F. Arbeiter, D. Bernardi, M. Frisoni, S. Gordeev, et al., *J. Nucl. Eng.* 3 (4) (2022) 385–397, <https://doi.org/10.3390/jne3040025>.
- [7] M. Serrano, R. Hernández, D. Plaza, Assessment of SSTT Technology 2020, EUROfusion IDM EFDA_D_2NJ8LL v1.0. 2020. Available online: <https://idm.euro-fusion.org/default.aspx?uid=2MLMCM> (accessed on 1 October 2022).
- [8] SpaceClaim 3D software, url: <https://www.ansys.com/products/3d-design/ansys-spaceclaim>.
- [9] C.J. Werner, et al., MCNP Version 6.2 Release Notes (LA-UR-18-20808), Los Alamos National Laboratory, 2018. https://laws.lanl.gov/vhosts/mcnp.lanl.gov/pdf_files/la-ur-18-20808.pdf.
- [10] Y. Wu, Multi-functional neutronics calculation methodology and program for nuclear design and radiation safety evaluation, *Fusion Sci. Technol.* 74 (2018) 321–329.
- [11] Y. Wu, J. Song, H. Zheng, et al., CAD-based Monte Carlo program for integrated simulation of nuclear system SuperMC, *Ann. Nucl. Energy* 82 (2015) 161–168.
- [12] S.P. Simakov, U. Fischer, K. Kondo, P. Pereslavl'tsev, Status of the McDeLicious approach for the n-Li neutron source term modeling in IFMIF neutronics calculations, *Fusion Sci. Technol.* 62 (2012) 233–239.
- [13] A. Konobeyev, Yu. Korovin, P. Pereslavl'tsev, U. Fischer, U. Von Möllendorff, Development of methods for calculation of deuteron-lithium and neutron-lithium cross sections for energies up to 50 MeV, *Nucl. Sci. Eng.* 139 (2001) 1–23.
- [14] FENDL-3.1d: fusion evaluated nuclear data library Ver.3.1d, <https://www.nds.iaea.org/fendl/>.
- [15] M.C. White, “Further notes on MCPLIB03/04 and new MCPLIB63/84 compton broadening data for all versions of MCNP5,” Technical Report, LA-UR-12-00018, Los Alamos National Laboratory, 2012.
- [16] K. Nordlund, S.J. Zinkle, A.E. Sand, F. Granberg, R.S. Averback, et al., Improving atomic displacement and replacement calculations with physically realistic damage models, *Nat. Commun.* 9 (2018) 1084, <https://doi.org/10.1038/s41467-018-03415-5>.
- [17] G.R. Odette, P.J. Maziasz, J.A. Spitznagel, Fission–fusion correlations for swelling and microstructure in stainless steels: effect of the helium to displacement per atom ratio, *J. Nucl. Mater.* 103/104 (1981) 1289–1304.
- [18] F. Martín-Fuertes, M.E. García, P. Fernández, Á. Cortés, G. D'Ovidio et al. SC04.D005 - SC11.D012 - safety analysis report, version 2.0 (2PN9XX v0.0) (current) and the Update of irradiation and contamination areas verification [SC11.D006]. https://idm.euro-fusion.org/?uid=2PNKRF&version=v0.0&action=get_document.
- [19] D. Stork, P. Agostini, J.-L. Boutard, et al., Materials R&D for a timely DEMO: key findings and recommendations of the EU roadmap materials assessment group, *Fusion Eng. Des.* 89 (2014) 1586–1594.
- [20] M.R. Gilbert, S.L. Dudarev, S. Zheng, L.W. Packer, J.C. Sublet, An integrated model for materials in a fusion power plant: transmutation, gas production, and helium embrittlement under neutron irradiation, *Nucl. Fusion* 52 (2012) 083019, <https://doi.org/10.1088/0029-5515/52/8/083019>.